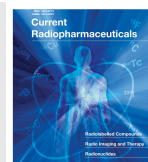




Cyclotron Production of PET Radiometals in Liquid Targets: Aspects and Prospects



Mukesh K. Pandey^{1,*} and Timothy R. DeGrado¹

¹Division of Nuclear Medicine, Department of Radiology, Mayo Clinic Rochester, Minneapolis, 55905, USA

ARTICLE HISTORY

Received: April 29, 2020
Revised: July 11, 2020
Accepted: July 23, 2020

DOI:
10.2174/1874471013999200820165734



CrossMark

This is an Open Access article published under CC BY 4.0
<https://creativecommons.org/licenses/by/4.0/legalcode>

Abstract: The present review describes the methodological aspects and prospects of the production of Positron Emission Tomography (PET) radiometals in a liquid target using low-medium energy medical cyclotrons. The main objective of this review is to delineate and discuss the critical factors involved in the liquid target production of radiometals, including type of salt solution, solution composition, beam energy, beam current, the effect of irradiation duration (length of irradiation) and challenges posed by in-target chemistry in relation with irradiation parameters. We also summarize the optimal parameters for the production of various radiometals in liquid targets.

Additionally, we discuss the future prospects of PET radiometals production in the liquid targets for academic research and clinical applications. Significant emphasis has been given to the production of ⁶⁸Ga using liquid targets due to the growing demand for ⁶⁸Ga labeled PSMA vectors, [⁶⁸Ga]-Ga-DOTATATE, [⁶⁸Ga]Ga-DOTANOC and some upcoming ⁶⁸Ga labeled radiopharmaceuticals. Other PET radiometals included in the discussion are ⁸⁶Y, ⁶³Zn and ⁸⁹Zr.

Key words: Liquid target, solution target, cyclotron, radiometals, ⁶⁸Ga, ⁸⁶Y, ⁶³Zn and ⁸⁹Zr.

1. INTRODUCTION

Cyclotron production of PET radiometals in a liquid target is an attractive approach due to the simplicity and ease of loading and unloading the target (isotope transfer). Decades of experience in the successful production of ¹⁸F isotope in a liquid target supports this concept. However, the in-target chemistry during radiometals production in a liquid target is tremendously more complex than that of liquid target production of ¹⁸F. Therefore, in spite of its alluring approach, liquid target production of PET radiometals was a farfetched goal until very recently. Early attempts to produce radiometals in liquid targets revealed the challenges in making a usable quantity of radiometals [1-4]. Vogg *et al.* in 2004 produced ⁸⁶Y using naturally occurring strontium salt in an aqueous solution by irradiating the target solution for 60 min at 6 μA beam current. A yield of 21.6 MBq (0.58 mCi) of ⁸⁶Y was obtained at the end of the bombardment (EOB) in an open target system [1, 2]. Jensen *et al.* in 2011 used enriched [⁶⁸Zn]ZnCl₂ solution to produce ⁶⁸Ga from a cyclotron also in an open target system [3]. However, later other groups have attempted using the same enriched [⁶⁸Zn]ZnCl₂ solution in a closed system but failed due to foil rupture [5, 6]. DeGrado *et al.* in 2011 tried making ⁸⁹Zr in a solution target using an aqueous solution of yttrium nitrate with a cyclotron in a closed target system but observed extremely high in-target pressure [4]. The authors attributed

high target pressure to in-target electrolysis [4]. Hoehr *et al.* in 2012 showed cyclotron production of ^{99m}Tc using an aqueous solution of naturally occurring ⁹⁴Mo as either MoO₃ or as (NH₄)₆Mo₇O₂₄ dissolved in water and 30% hydrogen peroxide (H₂O₂). These authors showed 110±20 MBq (2.97±0.54 mCi) of highest yield of ^{99m}Tc at EOB with 60 min of target irradiation at 6 μA but also noted high in-target pressure [7, 8]. From these early studies, it was evident that liquid target production of radiometals was certainly different than routine ¹⁸F production in a liquid target. Radiometal production in liquid targets posed multiple challenges, including extremely high in-target pressure even at low beam current, low production yield, in-target precipitation, failure to run as a closed target system, inability to run at a high molar salt concentration or beam current and inability to perform long irradiations. Therefore, in spite of the alluring concept of radiometals production in a liquid target, it required fundamental work to understand the in-target chemistry to produce a usable quantity of radiometals for preclinical and clinical applications.

2. A MECHANISTIC APPROACH TO UNDERSTAND THE IN-TARGET CHEMISTRY

Initially, the main differences observed between ¹⁸F and radiometal production in liquid targets were the constant rise in in-target pressure and in-target precipitation of metal salts. These observations raised the question, what are the differences between ¹⁸F and radiometals target solutions? They both are aqueous solutions, but one contains salts in it and the other does not. This motivated Pandey *et al.* in 2014

*Address correspondence to this author at the Division of Nuclear Medicine, Department of Radiology, Mayo Clinic Rochester, Minneapolis, 55905, USA; E-mail: pandey.mukesh@mayo.edu

to perform a fundamental mechanistic study to understand the effect of the solution composition on in-target chemistry during ^{89}Zr production from naturally isotopically pure ^{89}Y salts [9]. In their study, they found that the rise in target pressure was caused by the formation of H_2 and O_2 gases due to the radiolysis of water. Interestingly, they also observed extremely high variation in gas evolution rates depending on the salt composition in the target [9]. For example, irradiation of aqueous solutions of NaCl , CaCl_2 , YCl_3 , NaNO_3 , $\text{Ca}(\text{NO}_3)_2$, and $\text{Y}(\text{NO}_3)_3$ at different concentrations gave the intriguing results shown in Fig. (1).

The rate of radiolysis of water was found to be several folds higher for the chloride salt of yttrium (YCl_3) relative to the nitrate salt $\text{Y}(\text{NO}_3)_3$, but this trend was completely reversed for the sodium salts with the highest gas evolution from NaNO_3 [9]. For calcium salts, the trend of overall gas evolved fell in between the above two, suggesting the role of the overall composition of the salt solution [9]. These observations indicated the effect of both cation and anion species (and their interactions within the irradiated solution) on the rate of radiolysis. For the case of $\text{Y}(\text{NO}_3)_3$ solution irradiations, a putative mechanism was proposed to explain how the nitrate ion may help to recombine $^{\circ}\text{OH}$ and H radicals as an H_2O and therefore mitigate gas evolution. In contrast, irradiation of YCl_3 solutions may lead to the formation of the intermediate ClOH^- that prevents the recombination of radicals from reforming water within the target [9]. Based on these findings, nitrate salt solutions were used for the production of various other radiometals like ^{68}Ga from $[\text{Zn}^{68}\text{Zn}(\text{NO}_3)_2]$ [10], ^{63}Zn from $[\text{Cu}^{63}\text{Cu}(\text{NO}_3)_2]$ [11], ^{64}Cu from $[\text{Ni}^{64}\text{Ni}(\text{NO}_3)_2]$ [12] ^{61}Cu from $[\text{Ni}^{61}\text{Ni}(\text{NO}_3)_2]$ [13] and ^{86}Y from $[\text{Sr}^{86}\text{Sr}(\text{NO}_3)_3]$ [14].

Pandey *et al.* also demonstrated that the presence of dilute nitric acid in yttrium nitrate salt solutions further reduces gas evolution by promoting recombination of $^{\circ}\text{OH}$ and H radicals as an H_2O [9]. In fact, a reduction in gas formation was also found with the YCl_3 solution on the addition of dilute nitric acid, further confirming the role of dilute nitric acid in suppressing the radiolysis of water [9]. The addition of dilute nitric acid not only reduced gas evolution but also helped to mitigate the in-target precipitation problem. The precipitate formed during irradiation of the yttrium nitrate solution in the absence of nitric acid was characterized as yttrium hydroxide. Therefore, precipitates formed during the production of other radiometals could also be expected to be the hydroxide salts of their corresponding parent metal ion. For example, for target solutions containing nitrate salts of Zn, Cu, Ni and Sr, the precipitates would be $\text{Zn}(\text{OH})_2$, $\text{Cu}(\text{OH})_2$, $\text{Ni}(\text{OH})_2$ and $\text{Sr}(\text{OH})_3$, respectively. Since these hydroxide salts have different aqueous solubilities, the amount of nitric acid required to prevent precipitation of these hydroxide salts during irradiation would also be different. The effects of beam current and irradiation duration are discussed in a later section.

In early 2020, Zacchia *et al.* also investigated the aspect of radiolysis in liquid target production of ^{89}Zr with an aim to further reduce the radiolysis of water and thus gas formation [15]. In their study, Zacchia *et al.* corroborated the use of nitrate salts and dilute nitric acid to have a viable liquid target system for radiometals production, and emphasized that it is the nitrate (NO_3) group that plays a critical role in mitigating radiolysis as described previously [9, 16]. One of the interesting findings of Zacchia *et al.* was that if the nitrate of the irradiating solution is reduced to nitrite (NO_2) salt prior to the irradiation, then it may further reduce the gas formation but only in the presence of dilute nitric acid or at acidic pH [15]. This gave further support of Pandey *et al.*'s suggestion that recombination of $^{\circ}\text{OH}$ and H radicals as an H_2O in a nitrate solution would proceed through the nitrite ion [9]. Additionally, varying the concentration of nitrite ions in dilute nitric acid did not change the rise in target pressure but there was a slight reduction in overall target pressure in comparison to use of the nitrate salt [15]. Although nitrite salts may lower target pressure during irradiation up to a certain extent, it poses a practical challenge to reduce every irradiating solution before production. The nitrite salt effect could be explained by an earlier approach to the steady-state target pressure due to the presence of nitrite ions to begin with. In the case of nitrate solutions, it may take some time to build up nitrite ions before reaching a steady-state target pressure. In spite of Zacchia *et al.*'s nitrite ion effect, the behavior of the pressure rise in the target was similar to that observed with the nitrate salts with the BMLT-2 target (Fig. 2) [16, 17].

3. THE EFFECT OF TARGET COOLING ON THE RATE OF RADIOLYSIS

The effect of solution composition was found as one of the most critical factors to reduce the in-target pressure and precipitation. However, enhanced cooling of liquid targets also plays a pivotal role in successful production of radiometals. A pictorial comparison of TS-1650 and BMLT-2 target designs are presented in (Fig. 3). Temperature gradients within the BMLT-2 target are lowered by cooling at the window foil (Havar) in addition to water cooling of the tantalum target body. The aluminum beam energy degrader foil is separately cooled by the helium flow. In contrast, the TS-1650 target, which was designed for ^{18}F production, was adapted to include a single 0.16 mm niobium foil (degrader and window together as a single foil versus the original 40 μm Havar foil) with no helium cooling [9, 10, 16]. Based on our experience, it is extremely critical to cool the window foil to avoid in-target precipitation. We have found precipitate on the window foil corresponding to the beam strike which is likely the hottest location within the target. Additionally, the conical shape of the BMLT-2 target body (Fig. 3) was designed to further enhance heat dissipation, and thus better mitigate the in-target pressure and precipitation [10, 16]. Enhanced cooling of the target attenuates the production of ionic and radical species and promotes the recombination of $^{\circ}\text{OH}$ and H radicals as an H_2O [9, 10]. The effect of target design and enhanced cooling was evident on ^{89}Zr production

yields in TS-1650 and BMLT-2 targets, as presented in Table 1 [16]. Various other radiometals were produced using the BMLT-2 target without any target pressure and precipitation issues [10, 11, 16, 17]. Again, we want to point

out that the TS-1650 target was designed for ^{18}F production only and not to produce radiometals. Therefore, the purpose of this comparison is only to emphasize the need for a specialized target design for radiometals production.

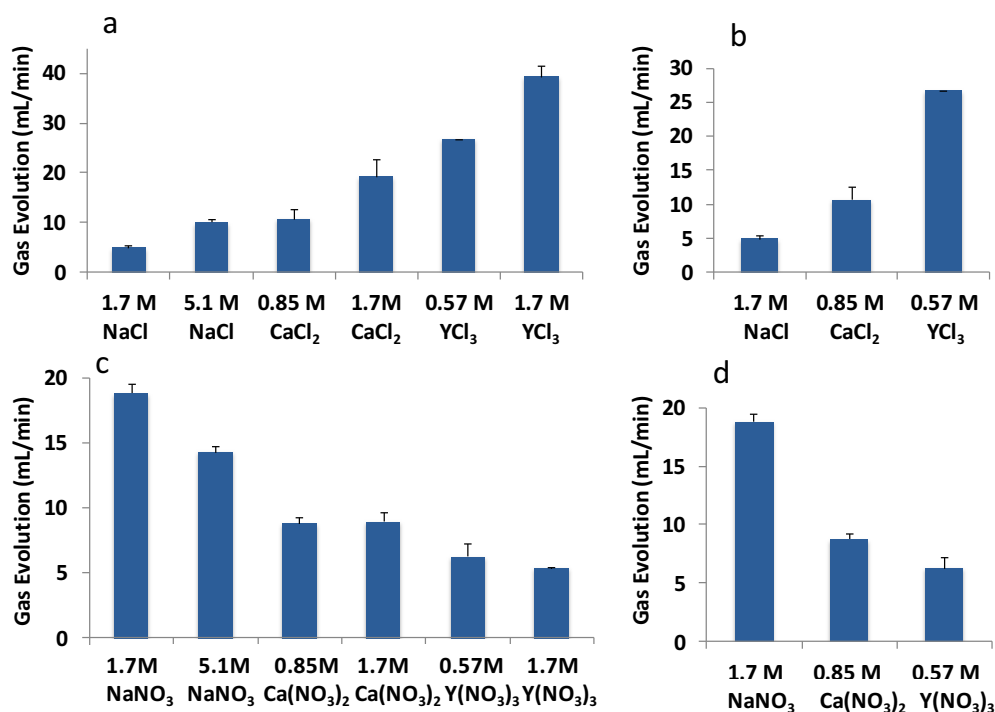


Fig. (1). Effect of solution composition on Gas evolution. (a) concentration of chloride salt; (b) cation at equal chloride content; (c) concentration of nitrate salt; (d) cation at equal nitrate content (figure is reproduced after permission from Elsevier Ref [9]). (A higher resolution / colour version of this figure is available in the electronic copy of the article).

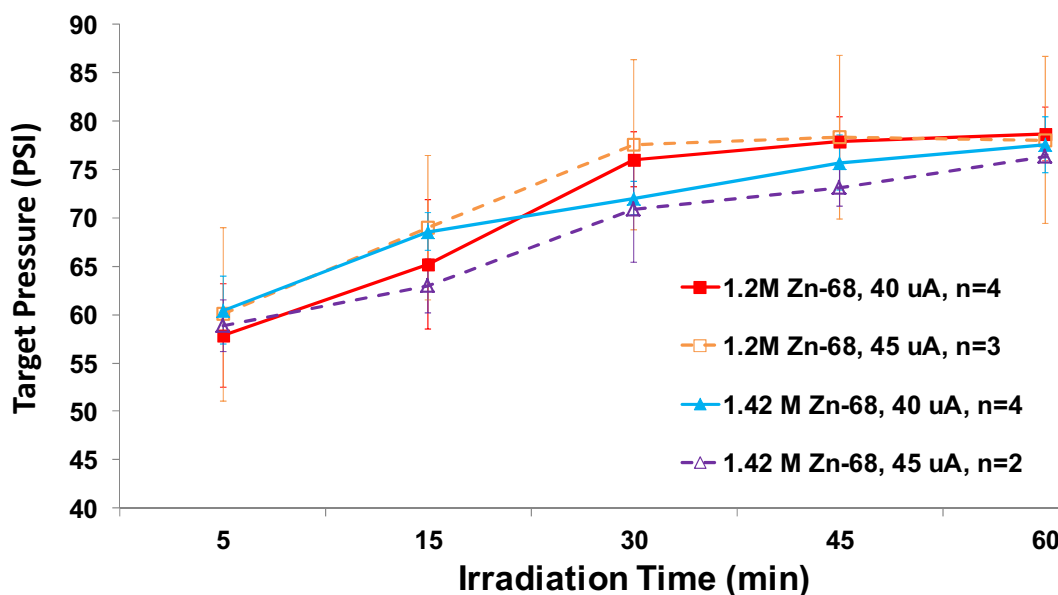


Fig. (2). Target pressure (PSI) during ^{68}Ga production at different proton beam currents and solution compositions. (Figure is reproduced after permission from Elsevier Ref [17]). (A higher resolution / colour version of this figure is available in the electronic copy of the article).

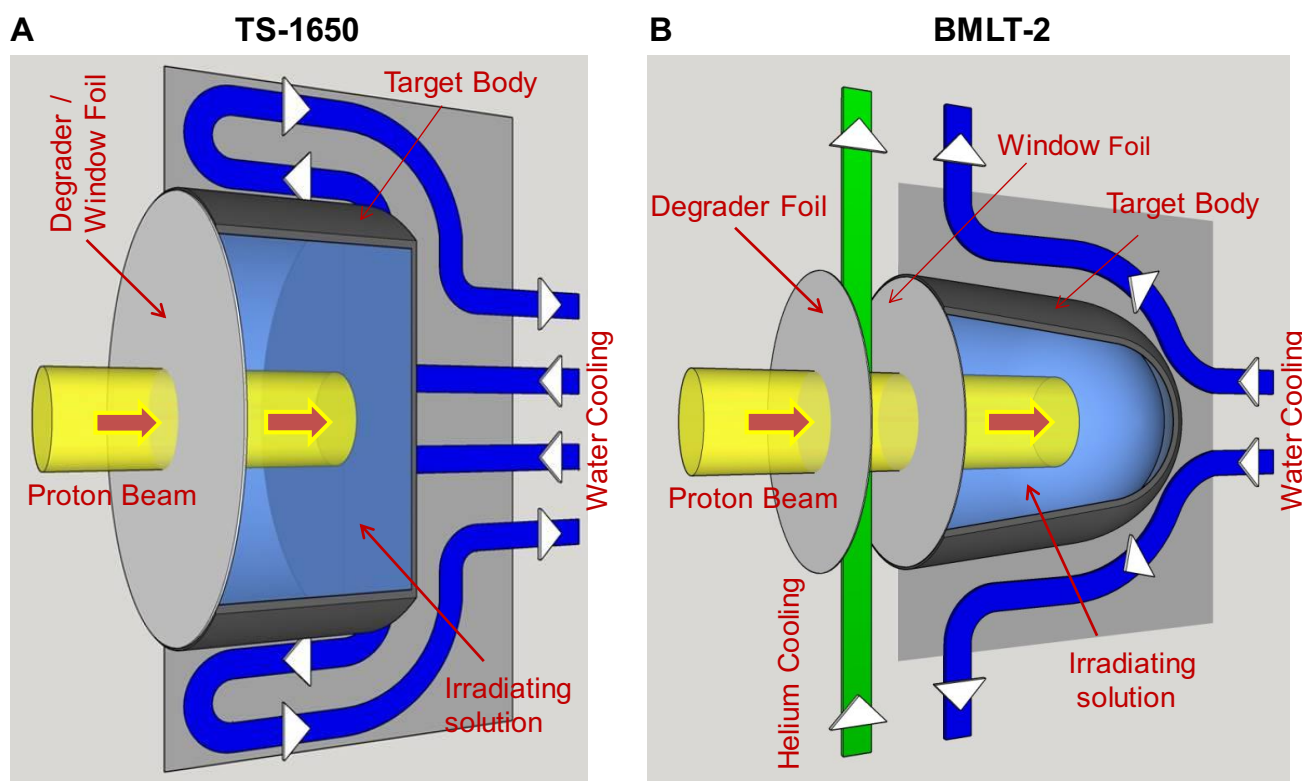


Fig. (3). Pictorial comparison of (A) TS-1650 and (B) BMLT-2 target designs and cooling systems. (A higher resolution / colour version of this figure is available in the electronic copy of the article).

Table 1. ^{89}Zr production rates in first and second-generation solution targets in comparison to a solid target. (Table is reproduced after permission from Elsevier ref [16]).

-	Molar concentration of $\text{Y}(\text{NO}_3)_3$ (M)	Beam Current (μA)	HNO_3 (M)	Decay Corrected EOB activity (MBq)	Production rate (MBq/ $\mu\text{A}\cdot\text{h}$)
TS-1650 target* (n=3)	2.75	20	1.50	153.1 \pm 15.1 (4.14 \pm 0.4 mCi)	3.82 \pm 0.37
BMLT-2 target (n=7)	2.00	40	1.25	348.8 \pm 48.7 (9.4 \pm 1.2mCi)	4.36 \pm 0.60
Solid target**	-	15	-	1664.63 (44.99 mCi)	53.28
Calculated yield***	-	-	-	-	43

*data from ref. [9], **data from ref. [23], *** data from ref. [30]

All irradiations were performed for 2h. Yields were calculated before isotope separation at the end of beam.

4. THE EFFECT OF IRRADIATION PARAMETERS ON IN-TARGET PRESSURE AND PRECIPITATION

It is important to consider the impact of irradiation parameters on the in-target chemistry and therefore radiometal production efficiency and reliability [17]. Typically, increasing beam current increases production yield but it also increases water radiolysis and subsequent in-target reactions which may lead to high gas evolution, and potentially, in-target salt precipitation. Optimal irradiation parameters depend upon multiple factors including individual target design, effective target cooling, solution composition and concentration (molarity of the salt solution). Therefore, it is critical to optimize production yield of radiometals as collective param-

eters not just as an individual parameter [17]. For example, in a recent study on ^{68}Ga production in a liquid target, increasing the beam current and irradiation duration increased ^{68}Ga production yield, but only after increasing the concentration of nitric acid (Fig. 4a & b) [17]. The findings indicated that the liquid target production of radiometals is a dynamic process with continuous consumption of nitric acid to maintain in-target solubility of the salt solution and recombination of $^{\circ}\text{OH}$ and H radicals as an H_2O . Besides, there may exist multiple interactions among the irradiation and solution composition parameters [17]. If one parameter is changed, it may affect the others and thereby affect production efficiency and reliability.

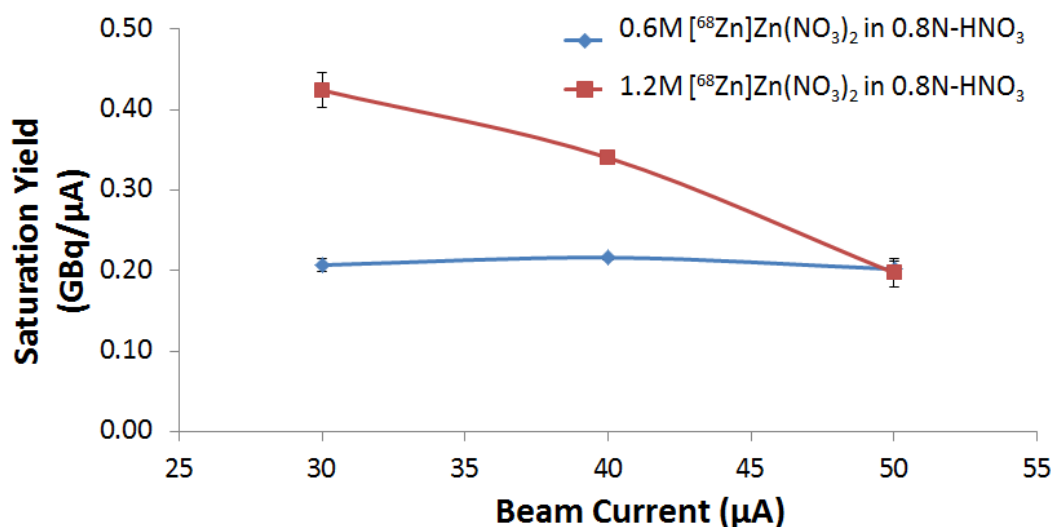


Fig. (4a). Effect of Zn-68 concentration and beam current at 0.8 N HNO₃, 30 min irradiation (Figure is reproduced after permission from Elsevier ref [17]). (A higher resolution / colour version of this figure is available in the electronic copy of the article).

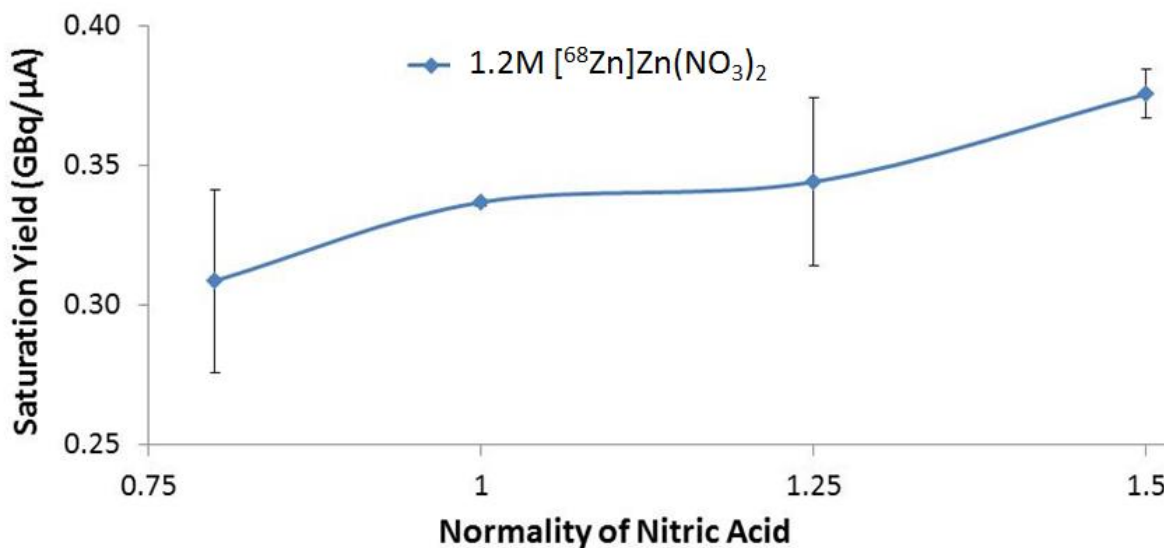


Fig. (4b). Effect of nitric acid on ⁶⁸Ga saturation yield at 30 μA at 60 min irradiation (Figure is reproduced after permission from Elsevier ref [17]). (A higher resolution / colour version of this figure is available in the electronic copy of the article).

5. EXCITATION CROSS SECTIONS FOR PROTON-INDUCED NUCLEAR REACTIONS IN LIQUID TARGETS

Since isotopically unenriched water (¹⁶O]H₂O, 55.5 mol/L) is the primary medium within target solutions in aqueous liquid targets, proton irradiations will produce a sizable quantity of ¹³N in the form of NO_x according to the ¹⁶O(p,α)¹³N cross section in low energy cyclotrons (Fig. 5A) [18]. Likewise, inclusion of dilute nitric acid in the liquid target solutions results in the production of [¹¹C]CO₂ according to the ¹⁴N(p,α)¹¹C cross section (Fig. 5B) [18]. Both of these radionuclides are shorter lived than the radiometals of interest and are readily separated by isotope separation methods

previously described. Depending on the concentration of ⁶³Cu, ⁶⁸Zn, ⁸⁶Sr or ⁸⁹Y metal salts present in the target solution, the production of ⁶³Zn, ⁶⁸Ga, ⁸⁶Y, ⁸⁹Zr are governed by their respective (p,n) nuclear reaction cross sections (Fig. 5C-E) [19-21]. In cyclotrons having proton energies higher than 14 MeV, it is necessary to use intervening foils to degrade the incident proton energy to 12.5-14 MeV to avoid production of undesired radionuclides *via* (p,2n) reactions. For example, the nuclear reaction ⁸⁹Y(p,2n)⁸⁸Zr is effectively mitigated in ⁸⁹Zr productions by limiting proton energy to below 14 MeV [9]. In the case of ⁸⁶Y production, there is co-production of stable ⁸⁵Sr and ⁸⁶Sr for proton energies below 15 MeV (Fig. 5E), but these are separable from ⁸⁶Y by chemical separation [22].

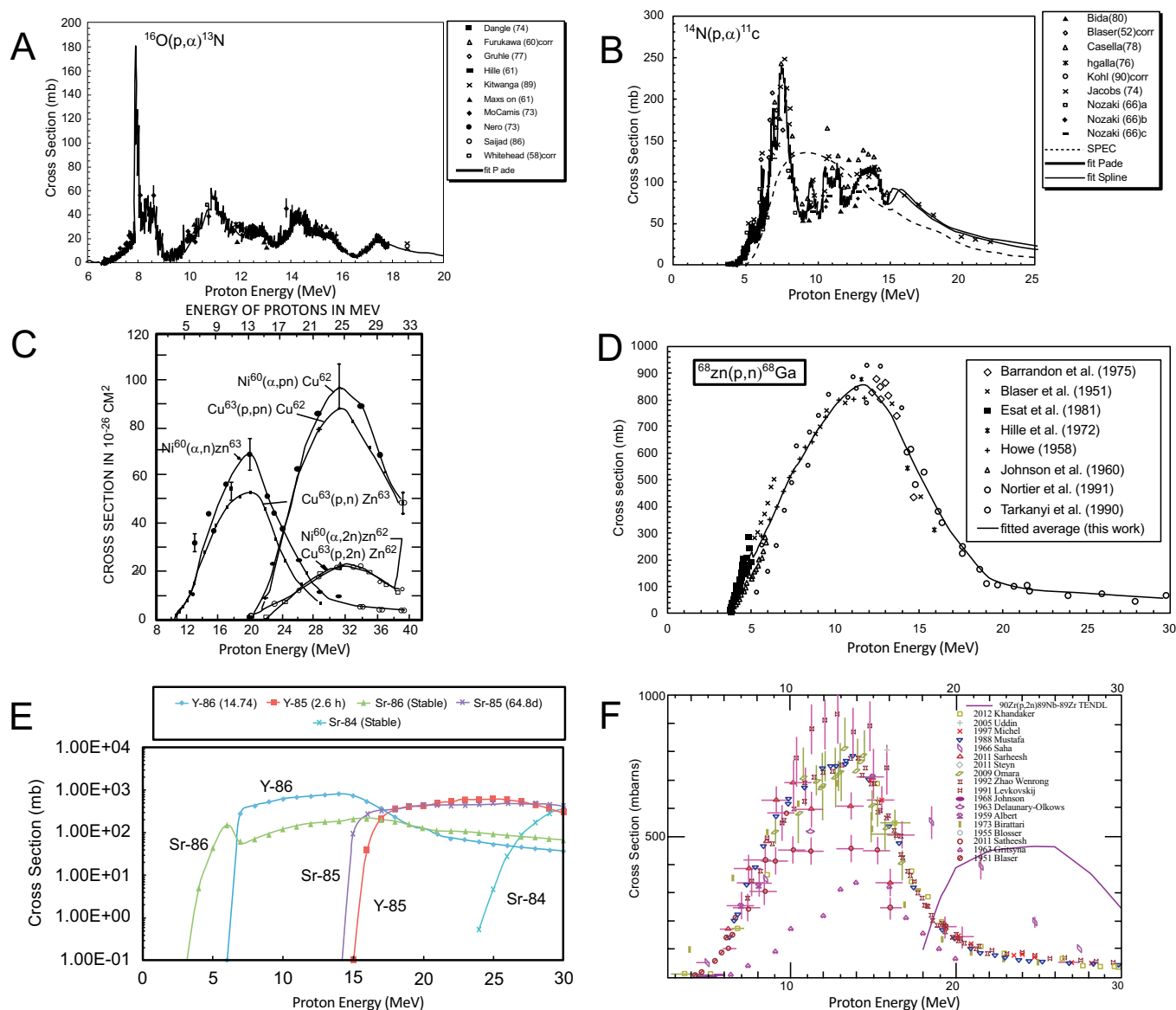


Fig. (5). Published excitation functions for (A) $^{16}\text{O}(p,\alpha)^{13}\text{N}$ [18]; (B) $^{14}\text{N}(p,\alpha)^{11}\text{C}$ [18]; (C) $^{63}\text{Cu}(p,n)^{63}\text{Zn}$ [19]; (D) $^{68}\text{Zn}(p,n)^{68}\text{Ga}$ [20]; (E) $^{86}\text{Sr}(p,n)^{86}\text{Y}$ [21] and (F) $^{89}\text{Y}(p,n)^{89}\text{Zr}$ [22]. (Figures A and B are reproduced after permission from IAEA for ref [18], figure C is reproduced after permission from APS for ref [19, <https://journals.aps.org/pr/abstract/10.1103/PhysRev.80.939>] and figures D, E and F are reproduced after permission from Elsevier publication for refs [20-22] (A higher resolution / colour version of this figure is available in the electronic copy of the article).

6. PRODUCTION OF VARIOUS RADIOMETALS ON THE CYCLOTRON USING A LIQUID TARGET

With fundamental understanding of the in-target chemistry in liquid targets, the production of various radiometals becomes feasible and relatively straight forward. However, depending upon the half-life and quantity of the radionuclide needed, optimization of the production parameters is necessary for each radionuclide. In the following, we have summarized successful production conditions, purification methods and major applications for ^{68}Ga , ^{86}Y , ^{63}Zn and ^{89}Zr .

6.1. ^{89}Zr Production, Purification and Application

^{89}Zr has emerged as a one of the most promising PET radionuclides for the labeling of monoclonal antibodies due to its imaging characteristics ($E_{\beta\text{max}}$ 0.9MeV, 22.7%) and favorable half-life ($T_{1/2}$ -78.4 h), which closely matches the clearance kinetics of monoclonal antibodies [9, 16]. Antibody based therapy and imaging are pivotal to understand the pathophysiology of various cancers. Due to relatively longer half-life of ^{89}Zr ($T_{1/2}$ -78.4 h), production of ^{89}Zr is more suited for a solid target using a cyclotron [23-25]. However, for

research and small-scale clinical applications, a liquid target can also be utilized for the production of ^{89}Zr [9, 15, 16, 20]. Pandey *et al.* have initially reported the successful production of ^{89}Zr using yttrium nitrate salts in dilute nitric acid [9]. In the same study, the authors have also demonstrated challenges associated with radiometals production in a liquid target due to water radiolysis. Addition of dilute nitric acid helped to mitigate both in-target pressure and precipitation, and allowed successful production of ^{89}Zr in a liquid target. However, in a later study to improve the ^{89}Zr production yield in the liquid target, the target design was changed to help dissipate the heat for enhanced cooling of the target solution. Enhanced cooling allowed irradiating the target at a higher beam current as a closed system, but higher concentrations of dilute nitric acid were needed to prolong the irradiation duration to 2h. Results obtained for the ^{89}Zr production in a liquid target are tabulated below [16]. The quality of ^{89}Zr produced from the liquid target approach was acceptable for biological studies [16, 26-29].

Purification of ^{89}Zr from Y-salt solutions using hydroxamate resin has been well established [16, 23]. However, final formulation of ^{89}Zr as a biocompatible solution has been explored differently. Final elution of ^{89}Zr from a hydroxamate resin was reported in the form of 1M oxalic acid solution [23]. Final formulation as [^{89}Zr]Zr-oxalate cannot be used directly in biological systems due to its toxicity, which has led to the development of other formulating/eluting solutions. Pandey *et al.* reported use of a biocompatible phosphate buffer to elute ^{89}Zr as [^{89}Zr]Zr(HPO_4)₂ from hydroxamate resin using 1.2 M $\text{K}_2\text{HPO}_4/\text{KH}_2\text{PO}_4$ at pH 3.5 [16]. Later Graves *et al.* reported tributyl phosphate (TBP)-functionalized extraction resin for the purification of ^{89}Zr from the Y-salt solution and final formulation as [^{89}Zr]ZrCl₄ using 0.1M HCl [31].

Whether ^{89}Zr is produced from a cyclotron using a solid target or liquid target, its application remains the same. However, due to the limited quantity of ^{89}Zr produced from a liquid target the application extent is limited as it cannot serve a larger number of routine patient studies. Nevertheless, a smaller number of patient studies are indeed possible with a 74-111 MBq (2-3 mCi) injection dose. Antibodies and cell labeling studies have been successfully conducted using cyclotron produced ^{89}Zr in a liquid target [26, 27].

6.2. ^{63}Zn Production, Purification and Application

Zinc plays a pivotal role in growth and development of the human body. Zinc is an essential micronutrient for proper functioning of the central nervous, immune, gastrointestinal, skeletal, and reproductive systems [32]. Recently, zinc ion dyshomeostasis has been implicated in various neurological diseases including Alzheimer's disease (AD), Parkinson's disease (PD) and Autism Spectrum Disorder (ASD) [11, 33]. PET imaging of zinc ion dyshomeostasis, zinc transport and abnormalities in zinc involving or containing pro-

teins can be instrumental in understanding the pathophysiology of various neurological and metabolic disorders.

There are three PET radionuclides of Zinc, ^{62}Zn ($T_{1/2}$, 9.26h), ^{63}Zn ($T_{1/2}$, 38.5 min) and ^{65}Zn ($T_{1/2}$, 243.9d). The long half-life of ^{65}Zn ($T_{1/2}$, 243.9d) precludes it for routine nuclear medicine applications. ^{62}Zn ($T_{1/2}$, 9.26h) decays to ^{62}Cu , another positron emitter (having half-life of 9.7 min), that may confound the image interpretations [11]. Therefore, ^{63}Zn ($T_{1/2}$, 38.5 min) remains the only option for routine clinical applications. ^{63}Zn can be produced from a cyclotron using both solid and liquid target systems [11, 34]. Production of ^{63}Zn using a solid target system was reported by Guerra-Gomez *et al.* in 2011 using a natural copper target [34]. De-Grado *et al.* 2014 reported production of ^{63}Zn from a cyclotron in a liquid target *via* the $^{63}\text{Cu}(p,n)^{63}\text{Zn}$ nuclear reaction using enriched ^{63}Cu nitrate salt in dilute nitric acid [11]. The production yield of ^{63}Zn from a cyclotron is tabulated below (Table 2).

Separation of ^{63}Zn from parent ^{63}Cu or ^{nat}Cu was reported by Guerra-Gomez *et al.* [34]. In brief, a cation exchange resin (Ag-50w-X8) was employed to selectively retain ^{63}Zn and pass through the parent isotope ^{63}Cu or ^{nat}Cu . Elution of ^{63}Zn from the cation exchange resin was carried out by a 0.05 N HCl-85% acetone solution. Acetone and hydrochloric acid were removed to dryness in a rotary evaporator and then reformulated in 5-10 mL water [34]. However, in order to make this process more feasible and practical for automation in a current good manufacturing practice (cGMP), De-Grado *et al.* employed a carboxymethyl (CM) cartridge and trapped ^{63}Zn on to a CM resin after neutralizing it with NaHCO_3 to remove acetone and HCl [11]. The final ^{63}Zn was eluted from the CM resin using 2-5 mL of USP grade 4% sodium citrate as a [^{63}Zn]Zn-citrate [11].

The same authors translated cyclotron-produced [^{63}Zn]Zn-citrate to humans after providing a cGMP method of producing [^{63}Zn]Zn-citrate and evaluation in a normal mouse model [34]. In their human study, they selected two cohorts, one including 6 healthy elderly individuals and other comprising 6 patients with clinically-confirmed Alzheimer's disease (AD). The hypothesis of the study was to find zinc imbalance in AD patients compared to healthy elderly patients using [^{63}Zn]Zn-citrate as a PET imaging probe of zinc transport in the brain [35]. Unfortunately, the uptake of ^{63}Zn -zinc citrate in the human brain was found to be relatively low compared to other brain imaging PET probes but it was noted that the kinetics of [^{63}Zn]Zn-citrate clearance in AD patients was slower than the healthy elderly cohort [35]. [^{63}Zn]Zn-citrate was also employed in a mechanistic study for kidney stone formation [36].

6.3. ^{86}Y Production, Purification and Application

The main advantage of ^{86}Y based PET imaging is the existence of ^{90}Y as a therapeutic partner. The ^{90}Y labeled anti-CD20 monoclonal antibody, [^{90}Y]Y- ibritumomab tiux-

Table 2. Production yield, specific activity and metal impurities in [⁶³Zn]Zn-citrate preparations (Reproduced from ref. [11] after permission).

Group	⁶³ Cu Used (mg/batch)	Conc. Of [⁶³ Cu]Cu (NO ₃) ₂ (M)	Batch yield after process* (GBq)	Saturated yield after process** (MBq/μA)	Specific Activity‡ (MBq / μg)	Metals (μg)
Non-cGMP	321 (n=3)	1.7	3.06±0.16	309±17	108±62 (36-144)	Fe ⁺³ : 13.0±2.1 Cu ⁺² : 40.5±16.1 Ni ⁺² : n.d. Zn ⁺² : 16.1±8.3
cGMP	232 (n=3)	1.23	1.88±0.44	160±17	34.2±13.8 (19.2 – 46.5)	Fe ⁺³ : 37.4±1.6 £ Cu ⁺² : 2.6±1.8 £ Ni ⁺² : n.d. Zn ⁺² : 25.2±1.4

All irradiations were at beam current of 20 μA for 60 min.

*decay corrected to EOB, processing time was ~36 min.

** decay corrected to EOB

‡At end of synthesis

£ Non-cGMP process, reused AG50W-X8 resin

† GMP process, new AG50W-X8 resin

£ p<0.05 versus

tan (Zevalin), was the first FDA-approved radioimmunotherapy agent or conjugated antibody for the treatment of non-Hodgkin lymphoma [37]. However, due to the lack of an imaging capability for ⁹⁰Y, a surrogate imaging isotope was needed to estimate the dosimetry and biodistribution of the therapeutic antibody. Initially, ¹¹¹In was used as an alternative due to the similar coordination number (3) for both yttrium (Y) and indium (In); however due to the difference in stability, biodistribution and kinetics of the complexes with yttrium and indium, a search continued until the emergence of ⁸⁶Y. Several radionuclides have been reported in the literature as “therapy-imaging pairs” to better understand the biodistribution and kinetics of the radiotherapy molecules as a surrogate to evaluate dosimetry [38, 39]. However, it has been evident that unless both imaging and therapy isotopes are of same element they are not truly a “therapy-imaging pair”. Differences in their stability, biodistribution and kinetics have been noticed, which has warranted routine production of ⁸⁶Y from a cyclotron [38]. The half-life of ⁸⁶Y is 14.7 h (β⁺ = 33%, E_{β⁺} mean= 0.6 MeV) and can be produced from a cyclotron using both solid and liquid targets. Production of ⁸⁶Y from a cyclotron was first reported by Rösch *et al.* in 1993 as [⁸⁶Y]Y-citrate [40]. Rösch *et al.* used enriched [⁸⁶Sr]SrCO₃ (96.3%) via a ⁸⁶Sr(p,n)⁸⁶Y nuclear reaction as the solid target material [40]. Later various other groups have produced ⁸⁶Y from a cyclotron using either enriched [⁸⁶Sr]Sr carbonate or oxide [41]. However, production of ⁸⁶Y from a cyclotron using a liquid target was first made in 2004 by Vogg *et al.* using natural strontium nitrate yielding 21.6 MBq of ⁸⁶Y decay corrected to EOB [1, 2]. After the introduction of nitrate salt and nitric acid as a combo for successful production of radiometals in a liquid target [9], Oehlke *et al.* in 2015 showed the feasibility of producing ⁸⁶Y using ^{nat}Sr(NO₃)₂ in 1M HNO₃, although with a low yield due to use of natural strontium nitrate as the solution for irradiation [5]. Later, as a proof of the concept, Pandey *et al.* in an International Atomic Energy Agency’s (IAEA) document presented use of isotopically enriched ⁸⁶Sr(NO₃)₂ (96%) in 0.2N-

HNO₃ for proton irradiation at 40 uA beam current for 30 min in a liquid target resulting in 337 MBq (9.11mCi) of [⁸⁶Y]YCl₃ post purification corrected to EOB [14].

Various methods have been developed over the years for separation of ⁸⁶Y from the parent isotope [38, 40-49] including using resin or column [38, 48, 49], electrolysis [41, 43, 47] or selective precipitation [44, 46]. The specific details of these separation methods have been recently summarized, compared and discussed by Rösch *et al.* [39]. For a liquid target, ⁸⁶Y was selectively precipitated by NH₄OH and retained on a Whatmen-42 filter paper as described previously [46]. Finally ⁸⁶Y was eluted from Whatmen-42 filter paper using 2 mL of a 1 M HCl solution as [⁸⁶Y]YCl₃ [14, 46].

Application of ⁸⁶Y as a true therapeutic partner for ⁹⁰Y based radiotherapeutics has been applied in imaging to evaluate dosimetry and biodistribution. Walrand *et al.* in 2003 employed ⁸⁶Y-DOTATATE imaging to identify the appropriate therapeutic dose for ⁹⁰Y-DOTATATE [50]. The presence of multiple single γ-rays from ⁸⁶Y other than the expected positron annihilation γ-rays led to significant overestimation of ⁸⁶Y-DOTATATE uptake, but this could be corrected by applying a patient-dependent sinogram tail fitting with a ⁸⁶Y point spread function library [50]. In spite of the clear potential of theranostic applications with ⁸⁶Y/⁹⁰Y radiopharmaceuticals they do not yet stand out as a mainstream choice. However, various preclinical studies are being published showing the importance and potential use of ⁸⁶Y based imaging in the future [51-65].

6.4. ⁶⁸Ga Production, Purification and Application

There is unabated interest in the clinical use of [⁶⁸Ga]Ga-DOTATATE for somatostatin receptor imaging in various cancers and ⁶⁸Ga labeled PSMA imaging in prostate and other non-prostate PSMA-positive cancer imaging. The ease of labeling and favorable imaging characteristics of ⁶⁸Ga (E_{pmax} 1.8 MeV, β+ 89%, T_{1/2} = 67.7 min) have made ⁶⁸Ga one

of the emerging radionuclides in clinical practice. The increased need for an on demand supply of ^{68}Ga is evident. Over the last two decades the supply of ^{68}Ga was dependent on $^{68}\text{Ge}/^{68}\text{Ga}$ generators, especially after the demonstration of ^{68}Ga elution with dilute hydrochloric acid [66]. However, the growing demand for ^{68}Ga on a routine basis has caused a significant wait time for institutions to acquire generators. In addition, scaling of the ^{68}Ga supply as per clinical need is not possible with the generator, and elution efficiency of the generator goes down over time. Need based availability of PET radionuclides is a standard norm in routine nuclear medicine practice, thus use of a cyclotron to produce ^{68}Ga becomes apparent. Application of a cyclotron to produce ^{68}Ga was first demonstrated by Sadeghi *et al.* in 2009 using a solid ^{68}Zn target [67, 68]. In 2011, Jensen *et al.* preliminarily reported a liquid target approach to produce ^{68}Ga on a cyclotron using an aqueous solution of $[\text{}^{68}\text{Zn}]\text{ZnCl}_2$ [3] in an open target. Later in 2014, Pandey *et al.* produced ^{68}Ga in a liquid target using solutions of $[\text{}^{68}\text{Zn}]\text{Zn}(\text{NO}_3)_2$ in dilute nitric acid [10] and other groups have generally followed after the same approach [5, 6, 69, 70]. However, Oehlke *et al.* and Riga *et al.* reported rapid target foil rupture upon irradiation of the $^{68}\text{ZnCl}_2$ solution due to high in target pressure and corrosion of the window foil with chloride salt along with in target precipitation [5, 6]. As previously discussed, it is critical to optimize the solution composition and irradiation parameters for each radiometal production, including ^{68}Ga . In a recent study, Pandey *et al.* investigated the effect of solution composition and various irradiation parameters on ^{68}Ga production yield. Results from this study are presented in Table 3 [17, 71].

There are two main approaches reported in the literature for purification of ^{68}Ga from the parent ^{68}Zn : 1) using a cation exchange resin (AG-50W-X8) [10], or 2) using hydroxamate resin [17, 72-74]. Both methods are adequate for purification of ^{68}Ga from ^{68}Zn , but to provide a cGMP acceptable formulation, a second ion-exchange resin needed to be employed in addition to either of the above two resins. The choice for the second resin was quite diverse including, DGA [5], AG-1 X8 anion exchange resin [10, 17, 69], TK200 [70], UTEVA [75, 76] and CUBCX strong cation [77]. Recently, Pedersen *et al.* reported a liquid-liquid extraction of $[\text{}^{68}\text{Ga}]\text{GaCl}_3$ from $[\text{}^{68}\text{Zn}]\text{ZnCl}_2$ in a continuous flow separated by a membrane using 1: 2 ratio of *n*-butyl ether and trifluorotoluene [78].

Radionuclidic purity of the cyclotron produced ^{68}Ga depends on two main factors: 1) isotopic enrichment of the parent ^{68}Zn , and 2) combination of cross section and the energy of the proton beam used for irradiation. The two competitive nuclear reactions that can lead to the formation of ^{66}Ga ($T_{1/2}$ 9.48 h) and ^{67}Ga ($T_{1/2}$ 78 h) are $^{66}\text{Zn}(p,n)^{66}\text{Ga}$ and $^{68}\text{Zn}(p,2n)^{67}\text{Ga}$, respectively [17, 79]. Formation of ^{66}Ga depends upon the percentage of ^{66}Zn present in the enriched ^{68}Zn parent material. In contrast, formation ^{67}Ga depends upon cross section and the energy of the proton beam used for irradiation. As long as proton irradiations are performed under 14

MeV the formation of ^{67}Ga remains well below 1% for a 60 min irradiation. Increasing irradiation time may increase the relative percentage of impurities [17, 79]. Synthesis of $[\text{}^{68}\text{Ga}]\text{Ga-PSMA-HBED}$ using a cyclotron produced $[\text{}^{68}\text{Ga}]\text{GaCl}_3$ in a cGMP environment has been usefully reported and is being evaluated in humans for recurrent prostate cancer and hepatocellular carcinoma [17, 80].

Applications of ^{68}Ga labeled radiopharmaceuticals are quite wide with a continuous increase over the last several years. In order to understand the current trends and interest in ^{68}Ga labeled radiopharmaceuticals, we performed a search on clinicaltrials.gov and found >80 clinical trials registered (Table 4) [80]. All together there are twenty different ^{68}Ga labeled compounds which are being evaluated for different clinical indications (Table 4).

Among the listed radiopharmaceuticals, ^{68}Ga -labeled PSMA vectors are emerging as leading compounds for evaluation of prostate cancer. There are currently nineteen clinical trials being conducted using $[\text{}^{68}\text{Ga}]\text{Ga-PSMA-HBED-CC}$ for prostate cancer either for direct evaluation or in comparison with other existing PET probes. $[\text{}^{68}\text{Ga}]\text{Ga-PSMA-HBED-CC}$ and other ^{68}Ga -labeled PSMA vectors are also being evaluated in non-prostate PSMA positive cancers like hepatocellular carcinoma, thyroid gland carcinoma, breast, ovarian and lung cancers. The second leading compound on the list is $[\text{}^{68}\text{Ga}]\text{Ga-DOTATATE}$, which is being evaluated for somatostatin receptor positive endocrine and non-endocrine tumors including esthesioneuroblastoma, hemangioblastoma, medulloblastoma, paraganglioma, ganglioneuroblastoma, ganglioneuroma, metastatic neuroblastoma and pituitary adenoma. The third leading compound on the list is $[\text{}^{68}\text{Ga}]\text{Ga-DOTA-TOC}$ being evaluated in meningioma, somatostatin positive malignancies, and adult and childhood medulloblastomas. The next two leading are $[\text{}^{68}\text{Ga}]\text{Ga-DOTA-NOC}$ and $[\text{}^{68}\text{Ga}]\text{Ga-NODAGA-exendin-4}$. $[\text{}^{68}\text{Ga}]\text{Ga-DOTA-NOC}$ is being evaluated for neuroendocrine tumors, cardiac sarcoidosis, lymphoma, and hodgkin disease, whereas, $[\text{}^{68}\text{Ga}]\text{Ga-NODAGA-exendin-4}$ is being evaluated in diabetes. Another interesting compound is $[\text{}^{68}\text{Ga}]\text{Ga-FAPi-46}$, which is being evaluated in various cancers including breast, colon, lung, kidney, esophageal, gastric, ovarian, pancreatic, and head and neck, as well as in solid neoplasm uterine corpus cancer.

7. SELECTION BETWEEN SOLID AND LIQUID TARGETS FOR CYCLOTRON PRODUCTION OF RADIOMETALS

The selection between a solid target and a liquid target for the production of radiometals can be challenging as both methods have advantages and disadvantages. However, selection can be made based on four major factors: 1) solid and liquid target capabilities, 2) amount of isotope needed, 3) processing time versus half-life, and 4) cost of the parent isotopes. For example, if an institution has only solid or liquid target production capability then the best use of available resources is the simple answer. However, if an institution has both solid and liquid target production capabilities

Table 3. Optimized yields of ⁶⁸Ga production in solution target (reproduced from ref [17]).

Molarity of [⁶⁸ Zn]Zn(NO ₃) ₂	Irradiation Parameters	Concentration of HNO ₃	⁶⁸ Ga Yield at EOB GBq (mCi)	Saturation Yield* (GBq/μA)
1.2 M (n=8)	30 min at 45μA	0.8N-HNO ₃	3.7±0.20 (100±6.0)	0.31±0.02
1.2 M (n=2)	30 min at 30 μA	0.8N-HNO ₃	3.37±0.17 (91.0±4.6)	0.42±0.02
1.2 M (n=2)	60 min at 40 μA	1.2N-HNO ₃	7.21±1.59 (195±43)	0.39±0.09
1.42 M (n=5)	60 min at 40 μA	1.2N-HNO ₃	9.85±2.09 (266±57)	0.54±0.11

*Yields were calculated before isotope separation.

Table 4. List of various ⁶⁸Ga labeled radiopharmaceuticals currently in clinical evaluation. (Data is extracted from clinicaltrials.gov).

S. No	Name of the Radiopharmaceuticals	Clinical indication (Number of studies)	Remark
1.	[⁶⁸ Ga]Ga-PSMA-HBED-CC	Recurring prostate cancer (19), Hepatocellular carcinoma (3), Prostatic neoplasms (1), Ovarian cancer (1), Thyroid gland carcinoma (1)	PET/CT, one study with direct comparison to [¹¹ C]Choline,
	[⁶⁸ Ga]Ga-PSMA**	PSMA positive tumors including prostate cancer (2), breast and lung cancers (1)	PET/MR
2.	[⁶⁸ Ga]Ga-DOTA-TATE	<ul style="list-style-type: none"> • Meningioma (3), Metastatic castration resistant prostate cancer (1), CNS tumors: Esthesioneuroblastoma (1), Hemangioblastoma (1), Medulloblastoma (1), Paraganglioma (1), Pituitary adenoma (1), Neuroendocrine tumor (4), Ganglioneuroblastoma (1), • Ganglioneuroma (1), • Metastatic neuroblastoma (1) 	PET/CT, PET/MRI
3.	[⁶⁸ Ga]Ga-DOTA-TOC	<ul style="list-style-type: none"> • Meningioma (2), Somatostatin positive malignancies (1), Pituitary tumors (1), Neuroblastoma (1), Adult medulloblastoma (1), • Childhood medulloblastoma (1) 	PET/CT, PET/MRI
4.	[⁶⁸ Ga]Ga-DOTA-NOC	<ul style="list-style-type: none"> • Neuroendocrine tumor (1), Cardiac sarcoidosis (1), Lymphoma (1), • Hodgkin Disease (1) 	PET/CT, for Cardiac Sarcoidosis head to head comparison with [¹⁸ F]FDG
5.	[⁶⁸ Ga]Ga-DOLACGA	Liver reserve evaluation (1)	PET/CT, Phase-1 safety evaluation in healthy Volunteers
6.	[⁶⁸ Ga]Ga-NODGA-MJ9	Prostate cancer	PET/CT direct comparison to [¹⁸ F]FCH
7.	[⁶⁸ Ga]Ga-MAA (Macro-aggregated albumin)	[⁶⁸ Ga]Ga-MAA Distribution in PAE patients. (1)	PET/MRI PAE: Prostate Artery Embolization patients
8.	[⁶⁸ Ga]Ga-P16-093	Prostate cancer with biochemical recurrence (1)	PET/CT
9.	[⁶⁸ Ga]Ga-DOTA-NeoBOMB	Prostate adenocarcinoma and recurrent prostate cancer (1)	PET/MRI
10.	[⁶⁸ Ga]Ga-NODAGA-exendin-4	Diabetes Mellitus, Type 2 (2)	PET/CT
11.	[⁶⁸ Ga]Ga-F(ab')-Trastuzumab	Solid tumor (1)	PET/CT, biodistribution and dosimetry
12.	[⁶⁸ Ga]Ga-Citrate	Infection and Inflammation	PET/CT, comparison with [¹⁸ F]FDG
13.	[⁶⁸ Ga]Ga-FAPi-46 (fibroblast activation protein)	Breast carcinoma (1), Colon carcinoma (1), Esophageal carcinoma (1), Gastric carcinoma (1), Head and neck carcinoma (1), Kidney carcinoma (1), Lung carcinoma (1), Ovarian carcinoma (1), Pancreatic carcinoma (1), Solid neoplasm uterine corpus cancer (1)	PET/CT
14.	[⁶⁸ Ga]Ga-Carbon nanoparticle	Sensitivity and specificity of V/Q PET/CT for the diagnosis of pulmonary embolism (PE) (1)	PET/CT, in association with [⁶⁸ Ga]Ga-MAA
15.	[⁶⁸ Ga]Ga-NOTA-MSA	Carotid atherosclerosis (1)	PET/CT
16.	[⁶⁸ Ga]Ga-RM2 Gastrin-releasing peptide receptor (GRPR) antagonist BAY86-7548 labeled with Ga-68	High risk prostate cancer (2), breast cancer (1)	PET/CT

(Table 4) contd....

17.	[⁶⁸ Ga]Ga-Pentixafor	Neuroendocrine tumor (1)	PET/CT
18.	[⁶⁸ Ga]Ga-HA-DOTATATE	Giant Cell Arteritis (GCA) (1)	PET/CT
19.	[⁶⁸ Ga]Ga-DOTA-(RGD)2	Imaging of tumor microenvironment in patients With oropharyngeal head and neck squamous cell carcinoma (1)	PET/CT
20.	[⁶⁸ Ga]Ga-ECMN	Hypoxia imaging (1)	PET/CT

** Chemical form of PSMA was not disclosed.

then the combination of the half-life of isotope, amount of isotope needed, processing time and cost of the parent isotope should be considered in making the decision. A similar approach can be applied by any institution who wishes to acquire either solid or liquid target capability. It is important to note that radionuclides having a half-life higher than ~60 min are better suited for production on a cyclotron using a solid target system whereas radionuclides having shorter half-lives may be better suited for production using liquid target systems (Fig. 6). This is simply because radionuclides that have long half-lives require longer an irradiation time (several hours) incompatible with liquid targets, whereas radionuclides with shorter half-lives build up faster during irradiation and can be delivered quickly as a liquid solution to a hot cell for processing. Ideally, the processing chemistry should be fast (<90 min) for the shorter lived radionuclides. For commercial applications that require distribution of radiopharmaceuticals distant from the manufacturing site, the solid target approach is preferred. Lastly, the cost of the parent isotope is an important consideration as the amount of parent isotope is considerably higher for liquid targets. The ability to recycle the parent isotope is also a factor in the decision. There will be unavoidable losses in purification and recycling. In fact, the overall cost of radionuclide production also includes efficiency of recycling and personnel cost for performing the work.

7.1. Prospects of Cyclotron Production of Radiometals in a Liquid Target

Understanding and unraveling the key processes are necessary to advance any science to the next level. Solution target production of radiometals is no different. Deciphering the in-target chemistry in liquid targets remains a limiting factor in advancing the production of radiometals to the next level. Even though the density of the parent target material is fairly low in liquid targets compared to solid targets, we maintain that there is significant value to continue advancing the liquid target approach for radiometal production. We must continue to enhance our understanding of in-target chemistry and reflexively apply changes to the target design to further advance our production capabilities. The successes that have been made so far were only possible after mechanistic investigation of gas and precipitate formation, effects of solution composition, target cooling designs, and irradiation parameters. Various radiometals including, ^{61/64}Cu, ⁶⁸Ga, ⁸⁶Y, ⁶³Zn, and ⁸⁹Zr, have been successfully produced in useful amounts using liquid targets. Present production quantities of ⁶⁸Ga and ⁶³Zn are sufficient enough to meet institutional needs for basic research, preclinical studies and small scale clinical translations. Indeed, ⁶³Zn and ⁶⁸Ga have been successfully translated to human studies. [⁶³Zn]Zn-citrate and

[⁶⁸Ga]Ga-PSMA-HBED are being evaluated in Alzheimer's disease and recurrent prostate cancer, respectively. In fact, [⁶⁸Ga]Ga-PSMA-HBED is also being evaluated in hepatocellular carcinoma and has potential to be useful in various other non-prostate PSMA positive cancers as listed in Table 4. Commercial liquid targets are now available for ⁶⁸Ga. Two other radionuclides, ⁸⁶Y and ⁸⁹Zr, which have been successfully produced on a cyclotron using a liquid target, have significant potential to be translated into human studies, although their production yields in liquid targets are low compared to solid targets. Nevertheless, liquid targets may provide smaller quantities of these radiometals for preclinical and limited clinical studies. Two of the copper radionuclides, ⁶¹Cu and ⁶⁴Cu, have also been successfully produced on a cyclotron using liquid targets [12, 13, 69, 81-83]. However, optimization of production yield is still needed. ⁶¹Cu and ⁶⁴Cu ions may be useful as imaging probes in various metal homeostasis studies. The reader is directed to two other recent review articles on production of radiometals using low energy cyclotrons and potential applications [82, 83].

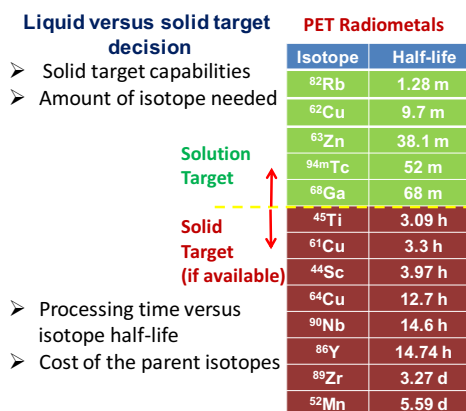


Fig. (6). Pictorial representation of selection of solid versus liquid targets for radiometals production. (A higher resolution / colour version of this figure is available in the electronic copy of the article).

CONCLUSION AND SUMMARY

An overview of the advancement of the liquid target approach of radiometals production on low energy cyclotrons from inception to present status has been presented. The current mechanistic understandings of the in-target chemistry and the effects of solution composition, target design and irradiation parameters have supported the production of useful quantities of ⁶⁸Ga, ⁸⁶Y, ⁶³Zn and ⁸⁹Zr radionuclides. Future prospects and current clinical applications of radiometals, in-

cluding a list of ^{68}Ga labeled radiopharmaceuticals under clinical evaluations, are also presented and discussed.

Technical terminology: For the ease of the reader, we define technical terminologies relevant to liquid targets for cyclotron production of radiometals.

- *Closed target system:* The closed target system means the target is isolated and hermetically sealed, meaning no exchange of liquid, vapor, or gas during irradiation. Both the lower inlet and upper outlet ports have lines that connect to a target loading unit that has high-pressure valves which are closed during the irradiation process. Thus, the lines between the target and the valves are technically included in the closed target system and may exchange mass of material (gas or liquid) with the target proper.
- *Open target system:* In an open target system, the upper outlet target port may be open to bleed off excess gasses produced during irradiation. This allows control of the target pressure but may lead to a lowering of production yield if the target material is lost from the target proper during irradiation.
- *Radiolysis:* Radiolysis is defined as the dissociation of molecules due to the ionizing radiation. In the case of water radiolysis, water molecules are broken down into multiple short-lived chemical species (radicals) by well-defined mechanisms and subject to variation with the addition of various additives [9, 84-86].
- *TS1650 target:* TS1650 is a standard F-18 production target, commercially available by the BTI Targetry, LLC.
- *BMLT2 target:* The BMLT-2 target is a prototype liquid target designed by the authors (Brigham and Women's Hospital, Boston, MA and Mayo Clinic, Rochester, MN).
- *Saturation yield:* Estimated maximal radionuclide production yield at saturation.

LIST OF ABBREVIATIONS

BMTL-2	= Brigham Mayo Liquid Target-2
cGMP	= current Good Manufacturing Practice; EOB, End of Bombardment
DOTA	= 1,4,7,10-tetraazacyclododecane-N,N',N'',N'''-tetraacetic Acid
DOTANOC	= DOTA-(1-NaI3)-octreotide
HBED	= N, N-bis(2-hydroxybenzyl)ethylenediamine-N,N-di-acetic Acid
PET	= Positron Emission Tomography
PSMA	= Prostate Specific Membrane Antigen; DOTATATE, DOTA-(Tyr ³)-octreotate

FUNDING

This work was supported financially by the Department of Energy (DOE) USA (Grant Number: DESC-0008947), The National Institute on Aging (NIA) USA (Grant Num-

ber: AG16574), The Center for Individualized Medicine, the Department of Radiology and the Mayo Clinic Alzheimer's Research Center, Mayo Clinic Rochester MN USA, and the Elsie and Marvin Dekelboum Family Foundation.

CONFLICT OF INTEREST

The authors have no conflict of interest, financial or otherwise.

ACKNOWLEDGMENTS

Authors would like to acknowledge and thank Mr. Jason Ellinghuysen for his support and help in drawing one of the figures (Fig. 3) in the present publication and Sonia Watson, PhD, in editing the manuscript.

REFERENCES

- [1] Vogg, A.T.J.; Lang, R.; Meier-Boeke, P.; Scheel, W.; Reske, S.N.; Neumaier, B. Cyclotron production of radionuclides in aqueous target matrices as alternative to solid state targetry: Production of Y-86 as example. *Proceedings of the sixth international conference on nuclear and radiochemistry*; Aachen, Germany, **2004**, 3, pp. 318-320.
- [2] Vogg, A.T.J.; Neumaier, B.; Scheel, W.; Reske, S.N. Access to remotely controlled production of ^{86}Y using aqueous target matrices as alternative to solid state targetry. *J. Label Compd. Radiopharm.*, **2005**, 48, S1-S341.
- [3] Jensen, M.; Clark, J. Direct production of Ga-68 from proton bombardment of concentrated aqueous solutions of $[\text{Zn-68}]$ zinc chloride. *Proceedings of 13th International Workshop on Targetry and Target Chemistry*, **2011**, pp. 288-292.
- [4] DeGrado, T.R.; Byrne, J.P.; Packard, A.B.; Belanger, A.P.; Rangarajan, S.; Pandey, M.K. A solution target approach for cyclotron production of Zr-89: Understanding and coping with in-target electrolysis. *J. Labelled Comp. Radiopharm.*, **2011**, 54, S248-S248.
- [5] Oehlke, E.; Hoehr, C.; Hou, X.; Hanemaayer, V.; Zeisler, S.; Adam, M.J.; Ruth, T.J.; Celler, A.; Buckley, K.; Benard, F.; Schaffer, P. Production of Y-86 and other radiometals for research purposes using a solution target system. *Nucl. Med. Biol.*, **2015**, 42(11), 842-849. <http://dx.doi.org/10.1016/j.nucmedbio.2015.06.005> PMID: 26264926
- [6] Riga, S.; Cicoria, G.; Pancaldi, D.; Zagni, F.; Vichi, S.; Dassenno, M.; Mora, L.; Lodi, F.; Morigi, M.P.; Marengo, M. Production of Ga-68 with a General Electric PETTrace cyclotron by liquid target. *Phys. Med.*, **2018**, 55, 116-126. <http://dx.doi.org/10.1016/j.ejmp.2018.10.018> PMID: 30473059
- [7] Hoehr, C.; Badesso, B.; Morley, T.; Trinczek, M.; Buckley, K.; Klug, J.; Zeisler, S.; Hanemaayer, V.; Ruth, T.R.; Benard, F.; Schaffer, P. Producing radiometals in liquid targets: Proof of feasibility with ^{94m}Tc . *AIP Conf. Proc.*, **2012**, 56, 1509.
- [8] Hoehr, C.; Morley, T.; Buckley, K.; Trinczek, M.; Hanemaayer, V.; Schaffer, P.; Ruth, T.; Bénard, F. Radiometals from liquid targets: ^{94m}Tc production using a standard water target on a 13 MeV cyclotron. *Appl. Radiat. Isot.*, **2012**, 70(10), 2308-2312. <http://dx.doi.org/10.1016/j.apradiso.2012.06.004> PMID: 22871432
- [9] Pandey, M.K.; Engelbrecht, H.P.; Byrne, J.P.; Packard, A.B.; DeGrado, T.R. Production of ^{89}Zr via the $^{89}\text{Y}(p,n)^{89}\text{Zr}$ reaction in aqueous solution: effect of solution composition on in-target chemistry. *Nucl. Med. Biol.*, **2014**, 41(4), 309-316. <http://dx.doi.org/10.1016/j.nucmedbio.2014.01.006> PMID: 24607433
- [10] Pandey, M.K.; Byrne, J.F.; Jiang, H.; Packard, A.B.; DeGrado, T.R. Cyclotron production of (^{68}Ga) via the $(^{68}\text{Zn}(p,n)^{68}\text{Ga})$ reaction in aqueous solution. *Am. J. Nucl. Med. Mol. Imaging*, **2014**, 4(4), 303-310. PMID: 24982816
- [11] DeGrado, T.R.; Pandey, M.K.; Byrne, J.F.; Engelbrecht, H.P.;

- Jiang, H.; Packard, A.B.; Thomas, K.A.; Jacobson, M.S.; Curran, G.L.; Lowe, V.J. Preparation and preliminary evaluation of ^{63}Zn -zinc citrate as a novel PET imaging biomarker for zinc. *J. Nucl. Med.*, **2014**, *55*(8), 1348-1354.
<http://dx.doi.org/10.2967/jnumed.114.141218> PMID: 25047329
- [12] Engelbrecht, H.; Byrne, J.; Packard, A.B.; Pandey, M.K.; Gruetz-macher, J.; DeGrado, T.R. Production of Cu-64 using a solution target. *J. Nucl. Med.*, **2013**, *54*(Suppl. 2), 1175.
<http://dx.doi.org/10.1148/radiol.2015150947> PMID: 26583911
- [13] Engelbrecht, H.; Pandey, M.K.; Packard, A.B.; Byrne, J.; DeGrado, T.R. Evaluating solution targetry for producing Cu-61 and Cu-64. *J. Labelled Comp. Radiopharm.*, **2013**, *56*, S38.
- [14] Production of emerging radionuclides towards theranostic applications: ^{43}Sc , ^{61}Cu , ^{86}Y . IAEA book in preparation **2020**.
- [15] Zacchia, N.A.; Martinez, D.M.; Hoehr, C. Radiolysis reduction in liquid solution targets for the production of ^{89}Zr . *Appl. Radiat. Isot.*, **2020**, *155*, 108791.
<http://dx.doi.org/10.1016/j.apradiso.2019.06.037> PMID: 31756554
- [16] Pandey, M.K.; Bansal, A.; Engelbrecht, H.P.; Byrne, J.F.; Packard, A.B.; DeGrado, T.R. Improved production and processing of ^{89}Zr using a solution target. *Nucl. Med. Biol.*, **2016**, *43*(1), 97-100.
<http://dx.doi.org/10.1016/j.nucmedbio.2015.09.007> PMID: 26471714
- [17] Pandey, M.K.; Byrne, J.F.; Schlasner, K.N.; Schmit, N.R.; DeGrado, T.R. Cyclotron production of ^{68}Ga in a liquid target: Effects of solution composition and irradiation parameters. *Nucl. Med. Biol.*, **2019**, *74-75*, 49-55.
<http://dx.doi.org/10.1016/j.nucmedbio.2019.03.002> PMID: 31085059
- [18] Tarkanyi, F.; Takacs, S.; Gul, K.; Hermanne, A.; Mustafa, M.G.; Nortier, F.M.; Oblozinsky, P.; Qaim, S.M.; Scholten, B.; Shubin, Y.N.; Zhuang, Y. Charged-particle cross section database for medical radioisotope production. *IAEA TEC*, **2001**, *DOC-1211*, 285.
- [19] Ghosal, S.N. An experimental verification of the theory of compound nucleus. *Phys. Rev.*, **1950**, *6*, 939-942.
<http://dx.doi.org/10.1103/PhysRev.80.939>
- [20] Szelecsenyi, F.; Boothe, T.E.; Takacs, S.; Tarkanyi, F.; Tavano, E. Evaluated cross section and thick target yield data bases of $\text{Zn} + p$ processes for practical applications. *Appl. Radiat. Isot.*, **1998**, *49*, 1005-1032.
[http://dx.doi.org/10.1016/S0969-8043\(97\)10103-8](http://dx.doi.org/10.1016/S0969-8043(97)10103-8)
- [21] Sadeghi, M.; Aboudzadeh, M.; Zali, A.; Zeinali, B. (86)Y production via (86)Sr(p,n) for PET imaging at a cyclotron. *Appl. Radiat. Isot.*, **2009**, *67*(7-8), 1392-1396.
<http://dx.doi.org/10.1016/j.apradiso.2009.02.038> PMID: 19285420
- [22] Tárkányi, F.; Ditrói, F.; Takács, S.; Hermanne, A.; Al-Abyad, M.; Yamazaki, H.; Baba, M.; Mohammadi, M.A. New activation cross section data on longer lived radio-nuclei produced in proton induced nuclear reaction on zirconium. *Appl. Radiat. Isot.*, **2015**, *97*, 149-169.
<http://dx.doi.org/10.1016/j.apradiso.2014.12.029> PMID: 25579457
- [23] Holland, J.P.; Sheh, Y.; Lewis, J.S. Standardized methods for the production of high specific-activity zirconium-89. *Nucl. Med. Biol.*, **2009**, *36*(7), 729-739.
<http://dx.doi.org/10.1016/j.nucmedbio.2009.05.007> PMID: 19720285
- [24] Wooten, A.L.; Madrid, E.; Schweitzer, G.D.; Lawrence, L.A.; Mebrahtu, E.; Lewis, B.C.; Lapi, S.E. Routine production of ^{89}Zr using an automated. *Appl. Sci. (Basel)*, **2013**, *3*, 593-613.
<http://dx.doi.org/10.3390/app3030593>
- [25] Alnahwi, A.H.; Tremblay, E.; Guerin, B. Comparative study with ^{89}Y -foil and ^{89}Y -pressed targets for the production of ^{89}Zr . *Appl. Sci. (Basel)*, **2018**, *8*, 1579.
<http://dx.doi.org/10.3390/app8091579>
- [26] Bansal, A.; Pandey, M.K.; Demirhan, Y.E.; Nesbitt, J.J.; Crespo-Diaz, R.J.; Terzic, A.; Behfar, A.; DeGrado, T.R. Novel (89)Zr cell labeling approach for PET-based cell trafficking studies. *EJN-MMI Res.*, **2015**, *5*, 19.
<http://dx.doi.org/10.1186/s13550-015-0098-y> PMID: 25918673
- [27] Yang, B.; Brahmhatt, A.; Nieves Torres, E.; Thielen, B.; McCall, D.L.; Engel, S.; Bansal, A.; Pandey, M.K.; Dietz, A.B.; Leof, E.B.; DeGrado, T.R.; Mukhopadhyay, D.; Misra, S. Tracking and therapeutic value of human adipose tissue-derived mesenchymal stem cell transplantation in reducing venous neointimal hyperplasia associated with arteriovenous fistula. *Radiology*, **2016**, *279*(2), 513-522.
<http://dx.doi.org/10.1148/radiol.2015150947> PMID: 26583911
- [28] Nicolas, C.T.; Hickey, R.D.; Allen, K.L.; Du, Z.; Guthman, R.M.; Kaiser, R.A.; Amiot, B.; Bansal, A.; Pandey, M.K.; Suksanpaisan, L.; DeGrado, T.R.; Nyberg, S.L.; Lilledag, J.B. Hepatocyte spheroids as an alternative to single cells for transplantation after ex vivo gene therapy in mice and pig models. *Surgery*, **2018**, *164*(3), 473-481.
<http://dx.doi.org/10.1016/j.surg.2018.04.012> PMID: 29884476
- [29] Bansal, A. Pandey, M.K.; Yamada, S.; Goyal, R.; Schmit, N.; Nesbitt, J.; Witt, T.; Singh, R.; Gunderson, T.; Boroumand, S.; Jeon, R.; Li, M.; Crespo-Diaz, R.; Hillestad, M.L.; Terzic, A.; Behfar, A.; DeGrado, T.R. [^{89}Zr]Zr-DBN labeled cardiopoietic stem cells proficient for heart failure. *Nucl. Med. Biol.*, **2020**, *90-91*, 23-30.
<http://dx.doi.org/10.1016/j.nucmedbio.2020.09.001>
- [30] Qaim, S.M. Development of novel positron emitters for medical applications: nuclear and radiochemical aspects. *Radiochim. Acta*, **2011**, *99*, 611-625.
<http://dx.doi.org/10.1524/ract.2011.1870>
- [31] Graves, S.A.; Kuttyreff, C.; Barrett, K.E.; Hernandez, R.; Ellison, P.A.; Happel, S.; Aluicio-Sarduy, E.; Barnhart, T.E.; Nickles, R.J.; Engle, J.W. Evaluation of a chloride-based ^{89}Zr isolation strategy using a tributyl phosphate (TBP)-functionalized extraction resin. *Nucl. Med. Biol.*, **2018**, *64-65*, 1-7.
<http://dx.doi.org/10.1016/j.nucmedbio.2018.06.003> PMID: 30015090
- [32] Roohani, N.; Hurrell, R.; Kelishadi, R.; Schulin, R. Zinc and its importance for human health: An integrative review. *J. Res. Med. Sci.*, **2013**, *18*(2), 144-157.
 PMID: 23914218
- [33] Barnham, K.J.; Bush, A.I. Biological metals and metal-targeting compounds in major neurodegenerative diseases. *Chem. Soc. Rev.*, **2014**, *43*(19), 6727-6749.
<http://dx.doi.org/10.1039/C4CS00138A> PMID: 25099276
- [34] Guerra-Gomez, F.L.G.; Takada, Y.; Hosoi, R.; Momosaki, S.; Yamamoto, K.; Nagatsu, K.; Suzuki, H.; Zhang, M.R.; Inoue, O.; Arano, Y.; Fukumura, T. Production and purification of the positron emitter zinc-63. *J. Labelled Comp., Radiopharm.*, **2012**, *55*, 5-9.
<http://dx.doi.org/10.1002/jlcr.1943>
- [35] DeGrado, T.R.; Kemp, B.J.; Pandey, M.K.; Jiang, H.; Gunderson, T.M.; Linscheid, L.R.; Woodwick, A.R.; McConnell, D.M.; Fletcher, J.G.; Johnson, G.B.; Petersen, R.C.; Knopman, D.S.; Lowe, V.J. First PET Imaging Studies With ^{63}Zn -Zinc Citrate in Healthy Human Participants and Patients With Alzheimer Disease. *Mol. Imaging*, **2016**, *15*, 1536012116673793.
<http://dx.doi.org/10.1177/1536012116673793> PMID: 27941122
- [36] Landry, G.M.; Furrow, E.; Holmes, H.L.; Hirata, T.; Kato, A.; Williams, P.; Strohmaier, K.; Gallo, C.J.R.; Chang, M.; Pandey, M.K.; Jiang, H.; Bansal, A.; Franz, M.C.; Montalbetti, N.; Alexander, M.P.; Cabrero, P.; Dow, J.A.T.; DeGrado, T.R.; Romero, M.F. Cloning, function, and localization of human, canine, and *Drosophila* ZIP10 (SLC39A10), a Zn^{2+} transporter. *Am. J. Physiol. Renal Physiol.*, **2019**, *316*(2), F263-F273.
<http://dx.doi.org/10.1152/ajprenal.00573.2017> PMID: 30520657
- [37] Grillo-López, A.J. Zevalin: the first radioimmunotherapy approved for the treatment of lymphoma. *Expert Rev. Anticancer Ther.*, **2002**, *2*(5), 485-493.
<http://dx.doi.org/10.1586/14737140.2.5.485> PMID: 12382517
- [38] Garmestani, K.; Milenic, D.E.; Plascjak, P.S.; Brechbiel, M.W. A new and convenient method for purification of ^{86}Y using a Sr(II) selective resin and comparison of biodistribution of ^{86}Y and ^{111}In labeled Hereceptin. *Nucl. Med. Biol.*, **2002**, *29*(5), 599-606.
[http://dx.doi.org/10.1016/S0969-8051\(02\)00322-0](http://dx.doi.org/10.1016/S0969-8051(02)00322-0) PMID: 12088731
- [39] Rösch, F.; Herzog, H.; Qaim, S.M. The beginning and development of the theranostic approach in nuclear medicine, as exemplified by the radionuclide pair ^{86}Y and ^{90}Y . *Pharmaceuticals*

- (Basel), **2017**, 10(2), E56.
<http://dx.doi.org/10.3390/ph10020056> PMID: 28632200
- [40] Rösch, F.; Qaim, S.M.; Stöcklin, G. Production of the positron emitting radioisotope ^{86}Y for nuclear medical application. *Appl. Radiat. Isot.*, **1993**, 44, 677-681.
[http://dx.doi.org/10.1016/0969-8043\(93\)90131-S](http://dx.doi.org/10.1016/0969-8043(93)90131-S)
- [41] Yoo, J.; Tang, L.; Perkins, T.A.; Rowland, D.J.; Laforest, R.; Lewis, J.S.; Welch, M.J. Preparation of high specific activity (^{86}Y) using a small biomedical cyclotron. *Nucl. Med. Biol.*, **2005**, 32(8), 891-897.
<http://dx.doi.org/10.1016/j.nucmedbio.2005.06.007> PMID: 16253815
- [42] Finn, R.D.; McDevitt, M.; Ma, D.; Jurcic, J.; Scheinberg, D.; Larson, S.; Shoner, S.; Link, J.; Krohn, K.; Schlyer, D. Low energy cyclotron production and separation of yttrium-86 for evaluation of monoclonal antibody pharmacokinetics and dosimetry. *Proceedings of the 15th International Conference*, Woodbury, NY **1999**, , pp. 991-993.
<http://dx.doi.org/10.1063/1.59302>
- [43] Reischl, G.; Rösch, F.; Machulla, H.-J. Electrochemical separation and purification of yttrium-86. *Radiochim. Acta*, **2002**, 90, 225-228.
http://dx.doi.org/10.1524/ract.2002.90.4_2002.225
- [44] Ketterer, K.; Linse, K.-H.; Spellerberg, S.; Coenen, H.H.; Qaim, S.M. Radiochemical studies relevant to the production of ^{86}Y and ^{88}Y at a small-sized cyclotron. *Radiochim. Acta*, **2002**, 90, 845-849.
http://dx.doi.org/10.1524/ract.2002.90.12_2002.845
- [45] Park, L.S.; Szajek, L.P.; Wong, K.J.; Plascjak, P.S.; Garmestani, K.; Googins, S.; Eckelman, W.C.; Carrasquillo, J.A.; Paik, C.H. Semi-automated ^{86}Y purification using a three-column system. *Nucl. Med. Biol.*, **2004**, 31(2), 297-301.
<http://dx.doi.org/10.1016/j.nucmedbio.2003.07.002> PMID: 15013497
- [46] Avila-Rodriguez, M.A.; Nye, J.A.; Nickles, R.J. Production and separation of non-carrier-added ^{86}Y from enriched ^{86}Sr targets. *Appl. Radiat. Isot.*, **2008**, 66(1), 9-13.
<http://dx.doi.org/10.1016/j.apradiso.2007.07.027> PMID: 17869530
- [47] Lukic, D.; Tamburella, C.; Buchegger, F.; Beyer, G.-J.; Comor, J.J.; Seimbille, Y. High efficiency production and purification of ^{86}Y based on electrochemical separation. *Appl. Radiat. Isot.*, **2009**, 67(4), 523-529.
<http://dx.doi.org/10.1016/j.apradiso.2008.12.008> PMID: 19181533
- [48] Kandil, S.A.; Scholten, B.; Hassan, K.F.; Hanafi, H.A.; Qaim, S.M. A comparative study on the separation of radioyttrium from Sr- and Rb-targets via ion-exchange and solvent extraction techniques, with special reference to the production of no-carrier-added ^{86}Y , ^{87}Y and ^{88}Y using a cyclotron. *J. Radioanal. Nucl. Chem.*, **2009**, 279, 823-832.
<http://dx.doi.org/10.1007/s10967-008-7407-0>
- [49] Medvedev, D.G.; Mausner, L.F.; Srivastava, S.C. Irradiation of strontium chloride targets at proton energies above 35 MeV to produce PET radioisotope Y-86. *Radiochim. Acta*, **2011**, 99, 755-761.
<http://dx.doi.org/10.1524/ract.2011.1880>
- [50] Walrand, S.; Jamar, F.; Mathieu, I.; De Camps, J.; Lonneux, M.; Sibomana, M.; Labar, D.; Michel, C.; Pauwels, S. Quantitation in PET using isotopes emitting prompt single gammas: application to yttrium-86. *Eur. J. Nucl. Med. Mol. Imaging*, **2003**, 30(3), 354-361.
<http://dx.doi.org/10.1007/s00259-002-1068-y> PMID: 12634962
- [51] Nayak, T.K.; Brechbiel, M.W. ^{86}Y based PET radiopharmaceuticals: radiochemistry and biological applications. *Med. Chem.*, **2011**, 7(5), 380-388.
<http://dx.doi.org/10.2174/157340611796799249> PMID: 21711222
- [52] Huang, J.; Cui, L.; Wang, F.; Liu, Z. PET tracers based on (^{86}Y). *Curr. Radiopharm.*, **2011**, 4(2), 122-130.
<http://dx.doi.org/10.2174/1874471011104020122> PMID: 22191651
- [53] Biddlecombe, G.B.; Rogers, B.E.; de Visser, M.; Parry, J.J.; de Jong, M.; Erion, J.L.; Lewis, J.S. Molecular imaging of gastrin-releasing peptide receptor-positive tumors in mice using ^{64}Cu - and ^{86}Y -DOTA-(Pro1,Tyr4)-bombesin(1-14). *Bioconjug. Chem.*, **2007**, 18(3), 724-730.
<http://dx.doi.org/10.1021/bc0602811> PMID: 17378600
- [54] McQuade, P.; Miao, Y.; Yoo, J.; Quinn, T.P.; Welch, M.J.; Lewis, J.S. Imaging of melanoma using ^{64}Cu - and ^{86}Y -DOTA-ReC-CMSH(Arg11), a cyclized peptide analogue of alpha-MSH. *J. Med. Chem.*, **2005**, 48(8), 2985-2992.
<http://dx.doi.org/10.1021/jm0490282> PMID: 15828837
- [55] Wei, L.; Zhang, X.; Gallazzi, F.; Miao, Y.; Jin, X.; Brechbiel, M.W.; Xu, H.; Clifford, T.; Welch, M.J.; Lewis, J.S.; Quinn, T.P. Melanoma imaging using (^{111}In), (^{86}Y - and (^{68}Ga -labeled CHX-A''-Re(Arg11)CCMSH. *Nucl. Med. Biol.*, **2009**, 36(4), 345-354.
<http://dx.doi.org/10.1016/j.nucmedbio.2009.01.007> PMID: 19423001
- [56] Banerjee, S.R.; Foss, C.A.; Pullambhatla, M.; Wang, Y.; Srinivasan, S.; Hobbs, R.F.; Baidoo, K.E.; Brechbiel, M.W.; Nimmagadda, S.; Mease, R.C.; Sgouros, G.; Pomper, M.G. Preclinical evaluation of ^{86}Y -labeled inhibitors of prostate-specific membrane antigen for dosimetry estimates. *J. Nucl. Med.*, **2015**, 56(4), 628-634.
<http://dx.doi.org/10.2967/jnumed.114.149062> PMID: 25722448
- [57] Löfvqvist, A.; Humm, J.L.; Sheikh, A.; Finn, R.D.; Kozirowski, J.; Ruan, S.; Pentlow, K.S.; Jungbluth, A.; Welt, S.; Lee, F.T.; Brechbiel, M.W.; Larson, S.M. PET imaging of (^{86}Y -labeled anti-Lewis Y monoclonal antibodies in a nude mouse model: comparison between (^{86}Y) and (^{111}In) radiolabels. *J. Nucl. Med.*, **2001**, 42(8), 1281-1287.
 PMID: 11483692
- [58] Nayak, T.K.; Regino, C.A.; Wong, K.J.; Milenic, D.E.; Garmestani, K.; Baidoo, K.E.; Szajek, L.P.; Brechbiel, M.W. PET imaging of HER1-expressing xenografts in mice with ^{86}Y -CHX-A''-DTPA-cetuximab. *Eur. J. Nucl. Med. Mol. Imaging*, **2010**, 37(7), 1368-1376.
<http://dx.doi.org/10.1007/s00259-009-1370-z> PMID: 20155263
- [59] Nayak, T.K.; Garmestani, K.; Milenic, D.E.; Baidoo, K.E.; Brechbiel, M.W. HER1-targeted ^{86}Y -panitumumab possesses superior targeting characteristics than ^{86}Y -cetuximab for PET imaging of human malignant mesothelioma tumors xenografts. *PLoS One*, **2011**, 6(3), e18198.
<http://dx.doi.org/10.1371/journal.pone.0018198> PMID: 21464917
- [60] Nayak, T.K.; Garmestani, K.; Baidoo, K.E.; Milenic, D.E.; Brechbiel, M.W. Preparation, biological evaluation, and pharmacokinetics of the human anti-HER1 monoclonal antibody panitumumab labeled with ^{86}Y for quantitative PET of carcinoma. *J. Nucl. Med.*, **2010**, 51(6), 942-950.
<http://dx.doi.org/10.2967/jnumed.109.071290> PMID: 20484421
- [61] Schneider, D.W.; Heitner, T.; Aliche, B.; Light, D.R.; McLean, K.; Satozawa, N.; Perry, G.K.; Yoo, J.; Lewis, J.S.; Parry, R. In vivo biodistribution, PET imaging, and tumor accumulation of Y-86- and In-111-antimindin/RG-1, engineered antibody fragments in LNCaP tumor-bearing nude mice. *Int. J. Cancer*, **2011**, 128, 920-926.
- [62] Wong, K.J.; Baidoo, K.E.; Nayak, T.K.; Garmestani, K.; Brechbiel, M.W.; Milenic, D.E. Production of emerging radionuclides towards theranostic applications: ^{43}Sc , ^{61}Cu , ^{86}Y *IAEA, Book in Preparation*, **2011**, 1-61.
- [63] McDevitt, M.R.; Chattopadhyay, D.; Jaggi, J.S.; Finn, R.D.; Zanzonico, P.B.; Villa, C.; Rey, D.; Mendenhall, J.; Batt, C.A.; Njardarson, J.T.; Scheinberg, D.A. PET imaging of soluble yttrium-86-labeled carbon nanotubes in mice. *PLoS One*, **2007**, 2(9), e907.
<http://dx.doi.org/10.1371/journal.pone.0000907> PMID: 17878942
- [64] Cheal, S.M.; Xu, H.; Guo, H.-F.; Lee, S.-G.; Punzalan, B.; Chalasani, S.; Fung, E.K.; Jungbluth, A.; Zanzonico, P.B.; Carrasquillo, J.A.; O'Donoghue, J.; Smith-Jones, P.M.; Wittrup, K.D.; Cheung, N.V.; Larson, S.M. Theranostic pretargeted radioimmunotherapy of colorectal cancer xenografts in mice using picomolar affinity Y- or Lu-DOTA-Bn binding scFv C825/GPA33 IgG bispecific immunconjugates. *Eur. J. Nucl. Med. Mol. Imaging*, **2016**, 43(5), 925-937.
<http://dx.doi.org/10.1007/s00259-015-3254-8> PMID: 26596724
- [65] Palm, S.; Enmon, R.M., Jr; Matei, C.; Kolbert, K.S.; Xu, S.; Zan-

- zonico, P.B.; Finn, R.L.; Koutcher, J.A.; Larson, S.M.; Sgouros, G. Pharmacokinetics and Biodistribution of (86)Y-Trastuzumab for (90)Y dosimetry in an ovarian carcinoma model: correlative MicroPET and MRI. *J. Nucl. Med.*, **2003**, *44*(7), 1148-1155. PMID: 12843231
- [66] Razbash, A.A.; Sevastianov, Yu.G.; Krasnov, N.N.; Leonov, A.I.; Pavlekin, V.E. Germanium-68 row of products. *Proceedings of the 5th International Conference on Isotopes, 5ICI, Brussels, Belgium, Medimond, Bologna, April 25-29, 2005*.
- [67] Sadeghi, M.; Kakavand, T.; Rajabifar, S.; Mokhtari, L.; Nezhad, A.R. Cyclotron production of ^{68}Ga via proton-induced reaction on ^{68}Zn target *Nukleonika*, **2009**, *54*, 25-28.
- [68] Sadeghi, M.; Kakavand, T.; Mokhtari, L. Ghol- amzadeh . Z. Determination of ^{68}Ga production parameters by different reactions using ALICE and TALYS codes. *Pramana. J. Phys.*, **2009**, *72*, 335-341. <http://dx.doi.org/10.1007/s12043-009-0029-4>
- [69] Alves, F.; Alves, V.H.P.; Do Carmo, S.J.C.; Neves, A.C.B.; Silva, M.; Abrunhosa, A.J. Production of copper-64 and gallium-68 with a medical cyclotron using liquid targets. *Mod. Phys. Lett. A*, **2017**, *3217*, 1740013. <http://dx.doi.org/10.1142/S0217732317400132>
- [70] Nair, M.; Happel, S.; Eriksson, T.; Pandey, M.K.; DeGrado, T.R.; Gagnon, K. Cyclotron production and automated new 2-column processing of [^{68}Ga]/GaCl₃. *Eur. J. Nucl. Med. Mol. Imaging*, **2017**, *44*, S119-S956.
- [71] Pandey, M.K.; Schmit, N.R.; Byrne, J.; DeGrado, T.R. Effects of Solution Composition and Irradiation Parameters on ^{68}Ga Production in a Liquid Target using Cyclotron. *J. Nucl. Med.*, **2018**, *59*(1), S665.
- [72] Pandey, M.K.; Schmit, N.R.; McEarchern, J.M.; DeGrado, T.R. Improved Processing of Ga-68 produced from cyclotron in a solution target. *WTTC16: Proceedings of the 16th International Workshop on Targetry and Target Chemistry Santa Fe*; NM, USA29 August-1 September 2016AIP Conference proceedings, **2017**, 1845, .
- [73] Pandey, M.K.; Schmit, N.R.; McEarchern, J.M.; DeGrado, T.R. Hydroxamate Mediated Processing of ^{68}Ga Produced from Cyclotron in a Solution target. *J. Label. Compd. Radiopharm.*, **2017**, *60*, S111-S640.
- [74] Pandey, M.K.; Schmit, N.R.; Byrne, J.; Truong, P.; Gagnon, K.; Eriksson, T.; DeGrado, T.R. Automated Processing of Cyclotron Produced ^{68}Ga Using Hydroxamate Resin. *J. Nucl. Med.*, **2017**, *58*(Suppl. 1), 333.
- [75] Siikanen, J.; Valdovinos, H.; Hernandez, R.; Coarasa, A.; McGoron, A.; Sandell, A.; Barnhart, T.; Nickles, J. *Cyclotron produced Ga-66/68 with thermal diffusion-Assisted bulk separation and Ag50W-X8/UTEVA purification*; Lund University: Sweden, **2013**.
- [76] Lin, M.; Waligorski, G.J.; Lepera, C.G. Production of curie quantities of ^{68}Ga with a medical cyclotron via the $^{68}\text{Zn}(p,n)^{68}\text{Ga}$ reaction. *Appl. Radiat. Isot.*, **2018**, *133*, 1-3. <http://dx.doi.org/10.1016/j.apradiso.2017.12.010> PMID: 29272820
- [77] Alnahwi, A.H.; Tremblay, S.; Ait-Mohand, S.; Beaudoin, J.F.; Guérin, B. Automated radiosynthesis of ^{68}Ga for large-scale routine production using ^{68}Zn pressed target. *Appl. Radiat. Isot.*, **2020**, *156*, 109014. <http://dx.doi.org/10.1016/j.apradiso.2019.109014> PMID: 32056692
- [78] Pedersen, K.S.; Nielsen, K.M.; Fonsleta, J.; Jensen, M.; Zhuravlev, F. Separation of radiogallium from zinc using membrane-based liquid-liquid extraction in flow: Experimental and COSMO-RS Studies. *Solvent Extr. Ion Exch.*, **2019**, *37*(5), 376-391. <http://dx.doi.org/10.1080/07366299.2019.1646982>
- [79] Graves, S.; Engle, J.; Eriksson, T.; Gagnon, K. Dosimetry of cyclotron-produced [^{68}Ga] Ga-PSMA-11, [^{68}Ga] Ga-DOTA-TATE, and [^{68}Ga] Ga-DOTA-TOC. *J. Nucl. Med.*, **2018**, *59*(Suppl. 1), 1003. <https://clinicaltrials.gov/ct2/results?cond=&term=Ga68&country=&state=&city=&dist=> [Accessed 2020].
- [80] Alves, V.H.P.; Do Carmo, S.J.C.; Alves, F.; Abrunhosa, A.J. Automated Purification of Radiometals Produced by Liquid Targets. *Instruments*, **2018**, *2*, 17. <http://dx.doi.org/10.3390/instruments2030017>
- [81] do Carmo, S.J.C.; Scott, P.J.H.; Alves, F. Production of radiometals in liquid targets. *EJNMMI Radiopharm. Chem.*, **2020**, *5*(1), 2. <http://dx.doi.org/10.1186/s41181-019-0088-x> PMID: 31925619
- [82] Synowiecki, M.A.; Perk, L.R.; Nijssen, J.F.W. Production of novel diagnostic radionuclides in small medical cyclotrons. *EJNMMI Radiopharm Chem*, **2018**, *3*(1), 3. <http://dx.doi.org/10.1186/s41181-018-0038-z> PMID: 29503860
- [83] Wren, J. Steady-state radiolysis: effects of dissolved additives. *Nuclear Energy and the Environment. ACS Symposium Series*, **2010**, 1046, pp. 271-295. <http://dx.doi.org/10.1021/bk-2010-1046.ch022>
- [84] Horne, G.P.; Donoclift, T.A.; Sims, H.E.; Orr, R.M.; Pimblott, S.M. Multi-Scale Modeling of the Gamma Radiolysis of Nitrate Solutions. *J. Phys. Chem. B*, **2016**, *120*(45), 11781-11789. <http://dx.doi.org/10.1021/acs.jpcc.6b06862> PMID: 27779879
- [85] Yakabuskie, P.A.; Joseph, J.M.; Stuart, C.R.; Wren, J.C. Long-term γ -radiolysis kinetics of NO₃(-) and NO₂(-) solutions. *J. Phys. Chem. A*, **2011**, *115*(17), 4270-4278. <http://dx.doi.org/10.1021/jp200262c> PMID: 21469690